Colloidal Particles

DOI: 10.1002/anie.201105821

Wet-Chemical Synthesis of Amphiphilic Rodlike Silica Particles and their Molecular Mimetic Assembly in Selective Solvents**

*Jie He, Binyu Yu, Matt J. Hourwitz, Yijing Liu, Maria Teresa Perez, Jun Yang, and Zhihong Nie**

Nano- and micrometer-sized colloidal particles (CPs) with shape anisotropy (e.g., rod-shaped particles) and chemical heterogeneity (e.g., patchy particles) have attracted significant attention owing to their fascinating optical, electronic, and magnetic properties in materials sciences.[1–3] Self-assembly of such colloidal building blocks as "atoms" or "molecules" (so-called "colloidal molecules") into novel architectures or ordered ensembles provides new opportunities for engineering materials and devices with otherwise unattainable properties.[4,5] In particular, assembly of rodlike CPs with two or multiple blocks can potentially produce a variety of spectacular structures, which arise from the interplay and competition of the structural asymmetry of rods, the orientation, and phase segregation of blocks.[1a,6] Currently, the preparation of such segmented rodlike CPs mainly relies on templated electrochemical deposition,[7] galvanic replacement,[8] phase separation,[3f] chemical vapor deposition,[9] hot coordinating solvents method,[10] and cation-exchange reactions.[11] These approaches, however, are either limited to crystalline or conductive materials, or they require the use of templates. The synthesis of segmented rodlike particles from amorphous materials (e.g., SiO_2) still remains a challenge.

From the study of the assembly of colloidal molecules one can fundamentally learn and understand the general principles of atomic and molecular interactions using CPs as model systems,[1,12] and one can practically use the strategy known from the self-assembly of atoms or molecules as an inspiration for the design of new functional materials of CPs, such as nonconventional photonic crystals.[3d,13] Anisotropic rodlike CPs with hydrophilic and hydrophobic blocks are typical models for the investigation of assembly behaviors and molecular interactions of amphiphilic molecules (AMs).[8] The Mirkin group reported an inspiring example of template-directed assembly of two-segment gold-polypyrrole (Au-PPy) rods prepared by a templating method.[7a] The assembly of Au-PPy rods is driven by a delicate balance of templates, capillary forces, adhesion and polymer hydration effects; such rods, however, cannot self-assemble in selective solvents.[7a,14]

Herein, we report a general strategy to design and synthesize monodispersed amphiphilic silica rods (ASRs) with two segmented components by using a simple wet-chemical method. This template-free synthesis allows the independent control over the aspect ratio of rods and the length of each individual block. We also demonstrated the molecular mimetic self-assembly of ASRs into various structures including flower micelles, bundle micelles, star micelles, planar monolayers, and reverse micelles in selective solvents. This self-assembly is solely determined by the properties and volume fraction of the constituent blocks of rods and the nature of solvents. The diverse morphologies of the self-assembled structures are a result of the dimension, shape, and rigidity of the ASRs, and such structures cannot be obtained from organic AMs.

The synthetic strategy we developed for the preparation of ASRs was inspired by the recent work of Zhang et al. and Kuijk et al.[15] The one-pot synthesis involves the consecutive hydrolysis of two silica precursors, tetraethoxysilane (TEOS) and hexadecyltrimethoxysilane (HDTMOS), in *n*-pentanol in the presence of water/ethanol and structure-directing agent, polyvinylpyrrolidone (Figure 1 a). The hydrolysis and condensation of TEOS at the interface of water emulsions favored the anisotropic growth of silica rods with one end tightly bound to the surface of the emulsions.[15] The silica rods could further propagate to form "diblock" rods by adding the second silica precursor. As a demonstration of the synthesis of ASRs, TEOS was initially introduced to grow a hydrophilic block. Upon the addition of HDTMOS, the hydrophilic rods served as seeds to grow the second block; the continuous growth was initiated from the boundary of seed rod and water emulsion. The representative TEM and SEM images of ASRs in Figure 1 b–e clearly indicate two distinguished blocks of the asymmetric "diblock" rods. The hydrophilic blocks are rigid and solid, while the hydrophobic blocks are flexible and have a hollow tail-like shape (Figure 1 b–e). The hydrophobic tube-like block has a wall thickness of approximately 5 nm (see the Supporting Information). The introduction of hexadecyl groups to one block leads to the chemical asymmetry of two blocks. Energy-dispersive X-ray spectroscopy (EDX; Figure 1 f,g) shows the different chemical compositions of the two ends of the ASRs. The relative carbon concentration (compared with oxygen) of the hydrophobic block in ASR-4 is approximately 32 wt% (Figure 1 g), which is two times higher than that of the hydrophilic block owing to the presence of long alkyl chains.[16] The chemical inhomogeneity of ASRs was further confirmed by the preferential physical

[*] Dr. J. He, M. J. Hourwitz, Y. Liu, M. T. Perez, Prof. Z. Nie
Department of Chemistry and Biochemistry, University of Maryland
College Park, MD 20742 (USA)
E-mail: znie@umd.edu
B. Yu, Prof. J. Yang
Biomedical Engineering Graduate Program
The University of Western Ontario
London, ON N6A 5B9 (Canada)

[**] This work is supported by startup funds from the University of Maryland. We acknowledge the support of the Maryland Nano-Center and its NispLab. The NispLab is supported in part by the NSF as a MRSEC Shared Experimental Facility

Supporting information for this article is available on the WWW under http://dx.doi.org/10.1002/anie.201105821.

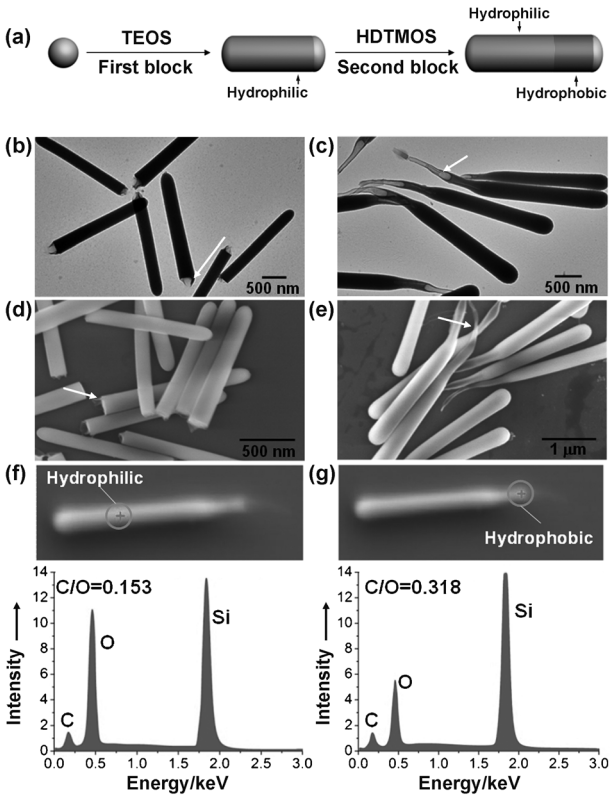

Figure 1. a) Schematic illustration of the synthesis of ASRs through consecutive hydrolysis and condensation of TEOS and HDTMOS. Hydrolysis of TEOS was first initiated at the surface of a water emulsion to induce anisotropic growth of the hydrophilic block. Upon the addition of HDTMOS, the growth of the hydrophobic second block continued at one end of the seed block. b–e) Representative TEM (b, c) and SEM (d, e) images of ASR-1 (b, d) and ASR-4 (c, e) show the asymmetric structures of rods (see Table 1 for the dimensions of ASR-1 and ASR-4). The arrow heads point at the hydrophobic ends of ASRs. f, g) EDX analysis of hydrophilic (f) and hydrophobic (g) blocks of ASR-4 indicates the chemical heterogeneity of ASRs.

absorption of a hydrophilic dye (rhodamine B) onto the hydrophilic block. Higher fluorescence intensity was observed in the hydrophilic block owing to the presence of more hydroxy groups in the hydrophilic block (see the Supporting Information).

Time-dependent growth of the hydrophobic block reveals a seed-mediated growth mechanism of segmented ASRs (Figure 2a–d; see the Supporting Information for the growth of the hydrophilic block).[15] The length of the hydrophobic block gradually increased during the reaction with HDTMOS, and reached up to approximately 1.8 μm in six hours. The wide openings at the hydrophobic ends of ASRs (highlighted by dashed cycles in Figure 2a) are believed to be the location of water emulsion where the hydrolysis of silica precursors occurred, as reported.[15b] The HDTMOS precursors cannot enter the center of water emulsion owing to its poor solubility in water. Therefore, the hydrolysis and condensation of HDTMOS is mainly localized at the emulsion–silica interface and results in the formation of hollow structures of the second block. A similar mechanism was also commonly observed in the growth of nanotubes (i.e., silica nanotubes) through chemical vapor deposition.[17] We further studied the growth kinetics of the hydrophobic block by monitoring the change in the chemical composition of each end of ASRs as the reaction proceeded. By using a confocal Raman microscope with a sub-micrometer resolution, Raman spectra of two ends of ASRs were recorded at different growth stages of the hydrophobic block (Figure 2b–d). Before the growth of the second block, Raman spectra of both ends were identical, thereby indicating the chemical symmetry of seed rods (Figure 2b). After the growth of the second block for 18 h, the intensities of peaks located at 2939 (C–H stretching) and 1450 cm^{-1} (C–H deformation) of one end of the rod were clearly higher than those of the other end. This intensity increase on one end further confirmed the formation of chemically asymmetric diblock structures (Figure 2c and see the Supporting Information). By using the peak of Si–O–Si stretching at 803 cm^{-1} as an internal standard, the relative intensity of the C–H stretching was calculated (see the Supporting Information) and plotted as a function of reaction time (Figure 2d).[18] The relative Raman intensity of C–H stretching can be quantitatively correlated to the amount of hexadecyl groups in individual rods, thus the approximate length of the hydrophobic block. The intensity increased with the increase of reaction time, thereby following a similar trend as the evolution of the hydrophobic length.

The seed-mediated synthesis of segmented silica rods allows us to independently tune the length of individual blocks and the ratios of hydrophilic length (L_1) to hydrophobic length (L_2), L_1/L_2 by varying the relative amount of silica precursors, TEOS and HDTMOS (Figure 2e). For example, the length of the hydrophilic block can be tuned from approximately 800 nm to 4 μm, and the length of the hydrophobic block can be changed from approximately 200 nm to 2 μm (see the Supporting Information). The optimal concentration range of HDTMOS was 20–80 μM, to avoid the secondary nucleation of HDTMOS and to produce monodispersed ASRs. The synthesized ASRs were used in all experiments without performing intentional purification to improve monodispersity. This method can be potentially extended to synthesize segmented rods with multiple blocks (see the Supporting Information) or with more complex patterns of functionality. This extension, however, is not the main focus of present work, and further research is currently undergoing.

The variation in the hydrophobicity, which originates from the chemical heterogeneity of individual blocks, enables the self-assembly of ASRs in selective solvents. By using rods denoted as ASR-1 to 4 (Table 1), we first studied the self-assembly of ASRs in polar water/ethanol mixtures to demonstrate the concept. The slow addition of water to ASRs dispersed in ethanol reduced the solubility of hydrophobic blocks of ASRs, thus leading to their spontaneous organization into various structures including flower micelles (Figure 3a), bundle micelles (Figure 3b), and star micelles (Figure 3c; see the Supporting Information for more SEM images). Analogous to organic AMs, the self-assembly of ASRs into micelles is mainly driven by the segregation of hydrophobic blocks (owing to the unfavorable mixing

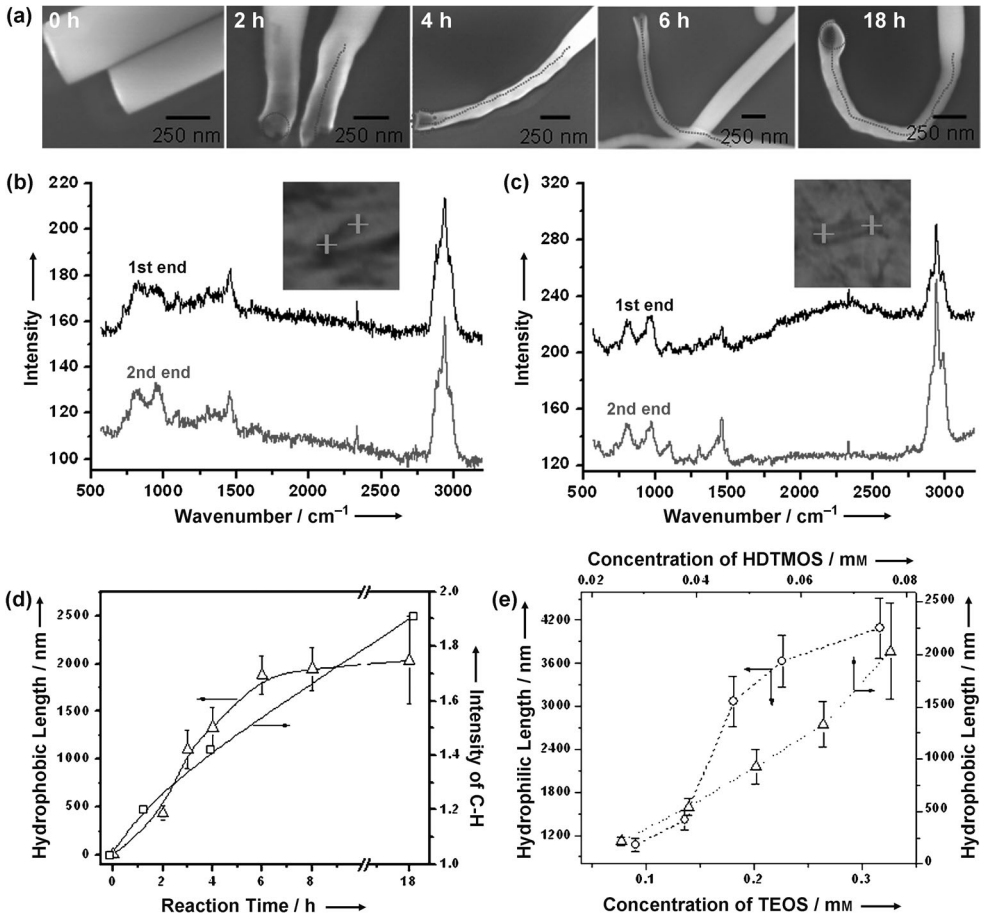

Figure 2. a) SEM images of the hydrophobic block of ASRs at different reaction times upon the addition of HDTMOS. The hydrophilic rods with a length of (3.04 ± 0.18) μm were used as seeds followed by addition of HDTMOS (35 μL) for the growth of the second blocks. Dashed lines indicate the pathways of the hydrophobic blocks. b,c) Typical confocal Raman spectra collected at two ends of ASRs 0 h (b) and 18 h (c) after the addition of HDTMOS. The inset optical images (9×9 μm) show the positions for collecting Raman spectra at each end of ASRs. The spectra were taken by focusing the laser beam (532 nm) with a submicrometer resolution at each end of the rods. d) The plot of the average length of hydrophobic blocks (△) and the relative Raman intensity (□) of C–H stretching at 2939 cm^{-1} (compared to Si–O–Si bending at 803 cm^{-1}) of two ends of ASRs as a function of reaction time. Each point of the average length of hydrophobic blocks was obtained by analyzing 50 rods. e) The dependence of the length of the hydrophilic (○, left and bottom axes) and hydrophobic (△, right and top axes) blocks on the amount of TEOS and HDTMOS, respectively. ○: [HDTMOS] = 51 μM. △: [TEOS] = 90 μM.

Table 1: Dimensions of ASRs used for self-assembly.

	L_1 [μm][a]	L_2 [μm][a]	d_1 [μm][b]	d_2 [μm][b]	L_1/L_2
ASR-1	1.81 ± 0.19	0.25 ± 0.04	0.21 ± 0.03	0.19 ± 0.05	7.2
ASR-2	1.01 ± 0.16	0.21 ± 0.03	0.36 ± 0.15	0.26 ± 0.09	4.8
ASR-3	2.25 ± 0.19	0.90 ± 0.23	0.30 ± 0.06	0.12 ± 0.03	2.5
ASR-4	2.40 ± 0.19	1.27 ± 0.16	0.34 ± 0.08	0.14 ± 0.05	1.9

[a] L_1 and L_2 are the average lengths of the hydrophilic and hydrophobic blocks, respectively. [b] d_1 and d_2 are the average diameters of hydrophilic and hydrophobic blocks, respectively. Diameter d_2 was obtained by averaging the diameters of the starting, middle, and end positions of hydrophobic blocks.

enthalpy).[19] Depending on the hydrophilic/hydrophobic balance (L_1/L_2), ASRs underwent two morphology transitions, varying their structures from flower micelles, to bundle micelles, and eventually to star micelles.

With a high length ratio of hydrophilic to hydrophobic blocks ($L_1 \gg L_2$), ASR-1 formed flower micelles with a low average aggregation number (N_{agg} ca. 3; Figure 3a). The aggregation number N_{agg} is calculated from $N_{agg} = \sum x_i N_i / \sum x_i$, where N_i is the i aggregation number in each assembled unit and x_i is number percentage. Dimers, trimers, and tetramers are the energy-favorable assemblies among all the aggregates (see the Supporting Information for SEM and fluorescence images). This preference is presumably due to the small enthalpy gain by aggregating the short hydrophobic blocks, and to the large steric effect that is caused by crowding of the rigid hydrophilic blocks in the vicinity of the hydrophobic cores. With increasing hydrophobic length, the diblock rods favored the formation of bundle micelles with hydrophilic blocks packed parallel to each other, which is rarely observed in organic AMs (see Figure 3b and the Supporting Information).[20] The preferential formation of bundle micelles is a result of the interplay of 1) minimizing the interfacial energy between the hydrophobic block and solvent and minimizing the elastic strain of the hydrophobic block by packing the rods side by side, and 2) an entropic penalty incurred for packing the rods side by side.[6,21] Compared to flower micelles, the average N_{agg} of bundle micelles is approximately 18. We have confirmed that the bundle micelles are formed from the self-assembly of rods in solution state rather than from the drying process, by using optical microscopy (see the Supporting Information). With the further increase of hydrophobic length, ASR-4 formed star micelles with the flexible hydrophobic blocks in the center of the micelle, while keeping the hydrophilic blocks in maximal contact with the surrounding polar solvent (Figure 3c and see the Supporting Information). The rounded interface can minimize the interfacial contact between the hydrophobic block and solvent. The rigid hydrophilic blocks were loosely packed around the hydrophobic core to form the soluble rod corona stabilizing the star micelles. The formation

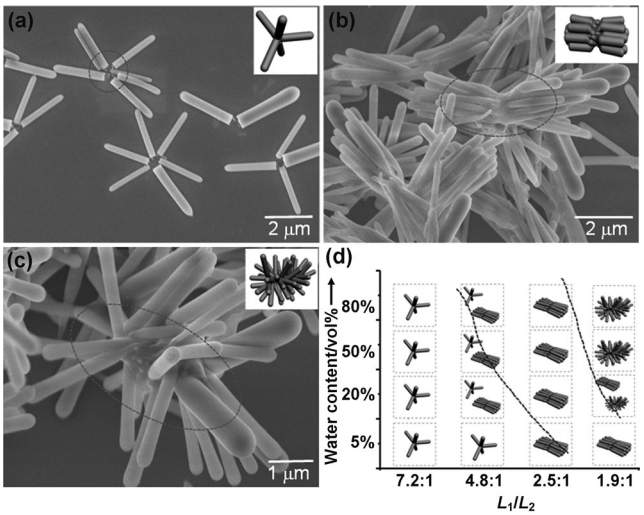

Figure 3. a–c) Typical SEM images of ASRs self-assembled in water/ethanol (1:1, vol) at a rod concentration of 5 mg mL^{-1}: a) ASR-1, flower micelles; b) ASR-3, bundle micelles; and c) ASR-4, star micelles. d) Phase-like diagram of the self-assembly of ASRs in water/ethanol by varying the length ratio, L_1/L_2 of hydrophilic block to hydrophobic block and water content. The dashed lines are drawn for eye guidance only.

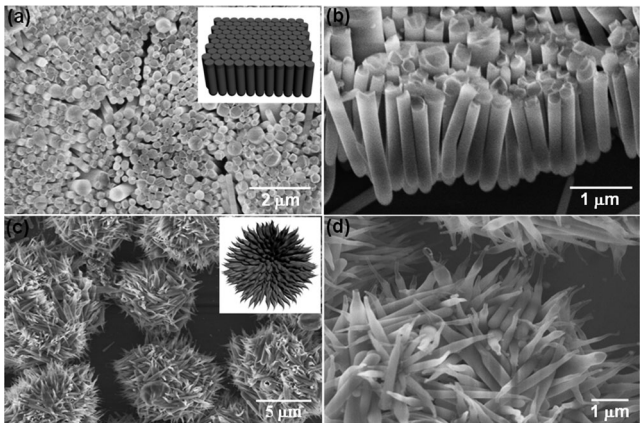

Figure 4. a–d) Typical SEM images of ASRs self-assembled in hexadecane/ethanol (8:2, vol) at a rod concentration of 10 mg mL^{-1}. a, b) Top (a) and side (b) view of planar monolayer assembled from ASR-1. Hydrophobic ends are at the top of the monolayer. c, d) Low- (c) and high- (d) magnification SEM images of reverse micelles obtained from ASR-4. Hydrophobic ends are pointing to the outside of the micelles.

of similar structures was predicted in computer simulation of the self-assembly of polymer-tethered nanorods in the selective solvent.[6]

Systematic study of the self-assembly of ASRs in water/ethanol is summarized in a phase-like diagram (Figure 3d). There are two morphology transitions in the current window of water concentration and L_1/L_2. By increasing water concentration and hydrophobic length, micellar aggregates of ASRs tend to transit from loose to dense packing, for example, from flower micelles to bundle micelles of ASR-2. However, this phase-like diagram does not cover regions in which ASRs comprise much longer hydrophobic length, owing to current synthetic challenge. The onset of ASR assembly is largely dependent on the concentration of rods.[19] For example, ASR-4 in water/ethanol (5:95, vol) mixture has a critical micelle concentration (CMC) of approximately 0.35 mg mL^{-1} (see the Supporting Information).

Self-assembly of ASRs can also be driven by apolar solvents. With the addition of apolar solvents, e.g., hexadecane, to ASRs in ethanol, ASRs self-assembled into 2D planar monolayers and reverse spherical micelles (Figure 4). In both cases, the hydrophilic blocks are densely packed to maximally avoid interaction with surrounding apolar solvents. ASR-1 and ASR-2 with short hydrophobic blocks formed 2D planar monolayers with lateral alignment of rods, and their hydrophobic ends pointed to the same direction (Figure 4a, b). The planar monolayer deposited onto various substrates with the long axis of the ASRs aligned perpendicular to the substrate. We observed that either side of the planar monolayers could face up when they were deposited on substrates, thereby indicating the formation of the self-assembled structures in solutions. The lateral dimensions of the planar monolayer ranged up to hundreds of micrometers. The formation of such morphology can be explained by minimization of the interfacial energy between the hydrophilic blocks and solvent through lateral packing and aligning of rods.[2e] We ascribe the formation of planar monolayers rather than that of bilayers, which present lower interfacial energy, to the limited contact between the rounded and rigid ends of hydrophilic blocks. The large-area vertical arrays of ASRs can be used as templates for the preparation of electrode materials for lithium batteries.[21] For ASR-3 and ASR-4 with long hydrophobic blocks, the hydrophilic blocks are forced to squeeze together, and the hydrophobic blocks are maximally exposed to the surrounding media to stabilize the structures. Reverse micelles were therefore obtained (Figure 4c, d). The extrusion of hydrophobic blocks of rods in the micelles mimics the rough surface of sweet-gum seeds. The diameter of reverse micelles ranged from 5 to 20 μm.

In summary, we developed a novel wet-chemical method to synthesize amphiphilic silica rodlike particles with rationally designed topologies and surface properties. This technique has at least three advantages over existing approaches: 1) it is a template-free method for synthesizing monodispersed rodlike particles with multiple segments; 2) it is a simple, fast, and facile approach to producing samples on a gram scale; and 3) this synthetic technique can potentially be extended to produce a library of CPs with more complex shapes and anisotropic functionalities as colloidal surfactants, as cargos for drug and gene delivery, and as building blocks for the construction of functional materials.[1,13] We further demonstrated that ASRs could spontaneously organize into diverse morphologies in solvents selective to constituent blocks. To our knowledge, this is the first report of the synthesis of the amphiphilic rodlike CPs by using a wet-chemical method and the first exploration of their self-assembly. The self-assembly of such ASRs could pave the way for studying phase behavior and packing of anisotropic CPs, and could serve as a new "visual" model for the dynamics of micell formation or biomimetic principles of self-organization observed in biological systems.[1,12]

Experimental Section

ASRs were synthesized through consecutive hydrolysis of two silica precursors. In a typical synthesis of rods with a hydrophilic length of 1.8 μm and a hydrophobic length of 0.2 μm, the detailed synthetic procedure is as follows. In a 20 mL glass vial, 1 g of polyvinylpyrrolidone (PVP, molecular weight 40 kg mol^{-1}) was dissolved in *n*-pentanol (10 mL) under sonication. Subsequently, deionized water (0.28 mL), anhydrous ethanol (1 mL), sodium citrate solution (0.1 mL, 180 mM in water), and ammonium hydroxide solution (0.17 mL, 28 wt %) were added to the above solution. The reaction mixture was vortexed for one minute to mix all the components. After the mixture was left standing for five minutes to release the gas bubbles, TEOS (0.06 mL) was added, and the solution was then gently shaken for 30 s. The hydrolysis of TEOS was allowed to proceed overnight at room temperature. After that, the hydrophobic monomer HDTMOS (0.03 mL) was added, and the mixture was again gently shaken. The hydrolysis of HDTMOS continued for another 12 h. The solution was then centrifuged at 6000 rpm for ten minutes, and the particles were washed five times with ethanol.

The self-assemblies of ASRs were imaged by using a Hitachi SU-70 Schottky field emission gun scanning electron microscope at an operation voltage of 5 kV. Samples for SEM were prepared by two methods: 1) casting ASR solution (10 μL) on silicon wafers, and 2) placing the silicon wafers at the bottom of a vial containing ASR solution for several minutes, then removing the silica wafers. The wafers were dried in air at room temperature. We did not observe obvious differences between samples prepared by these two approaches. TEM images were taken by using a JEOL 2100 LaB6 transmission electron microscope at an operation voltage of 200 kV. The Raman spectra and images of ASRs were recorded using a Horiba Yvon Lab Ram spectrometer equipped with a 532 nm laser. The spatial resolution (or the laser beam diameter) is down to sub-micrometer range.

Received: August 17, 2011
Revised: December 6, 2011
Published online: February 28, 2012

Keywords: amphiphiles · colloidal particles · micelles · self-assembly · silicium dioxide

[1] a) K. Liu, N. Zhao, E. Kumacheva, *Chem. Soc. Rev.* **2011**, *40*, 656; b) C. Burda, X. Chen, R. Narayanan, M. A. El-Sated, *Chem. Rev.* **2005**, *105*, 1025; c) Y. Xia, P. Yang, Y. Sun, Y. Wu, B. Mayers, B. Gates, Y. Yin, F. Kim, H. Yan, *Adv. Mater.* **2003**, *15*, 353; d) S. C. Glotzer, M. J. Solomon, *Nat. Mater.* **2007**, *6*, 557; e) M. J. Solomon, P. T. Spicer, *Soft Matter* **2010**, *6*, 1391; f) C. R. Martin, *Science* **1994**, *266*, 1961; g) F. Li, D. P. Josephson, A. Stein, *Angew. Chem.* **2011**, *123*, 378; *Angew. Chem. Int. Ed.* **2011**, *50*, 360; h) Z. W. Mao, H. L. Xu, D. Y. Wang, *Adv. Funct. Mater.* **2010**, *20*, 1053; i) V. J. Anderson, H. N. W. Lekkerkerker, *Nature* **2002**, *416*, 811; j) H. Zhang, E. W. Edwards, D. Y. Wang, H. Mohwald, *Phys. Chem. Chem. Phys.* **2006**, *8*, 3288.

[2] a) T. Mokari, E. Rothenberg, I. Popov, R. Costi, U. Banin, *Science* **2004**, *304*, 1787; b) M. Casavola, V. Grillo, E. Carlino, C. Giannini, F. Gozzo, E. F. Pinel, M. A. Garcia, L. Manna, R. Cingolani, P. D. Cozzoli, *Nano Lett.* **2007**, *7*, 1386; c) S. Deka, A. Falqui, G. Bertoni, C. Sangregorio, G. Poneti, G. Morello, M. De Giorgi, C. Giannini, R. Cingolani, L. Manna, P. D. Cozzoli, *J. Am. Chem. Soc.* **2009**, *131*, 12817; d) S. E. Habas, P. Yang, T. Mokari, *J. Am. Chem. Soc.* **2008**, *130*, 3294; e) N. Zhao, J. Vickery, G. Guerin, J. I. Park, M. A. Winnik, E. Kumacheva, *Angew. Chem.* **2011**, *123*, 4702; *Angew. Chem. Int. Ed.* **2011**, *50*, 4606; f) L. Manna, D. J. Milliron, A. Meisel, E. C. Scher, A. P. Alivisatos, *Nat. Mater.* **2003**, *2*, 382.

[3] a) M. G. Basavaraj, G. G. Fuller, J. Fransaer, J. Vermant, *Langmuir* **2006**, *22*, 6605; b) M. Grzelczak, J. Vermant, E. M. Furst, L. M. Liz-Marzan, *ACS Nano* **2010**, *4*, 3591; c) J. P. Singh, P. P. Lele, F. Nettesheim, N. J. Wagner, E. W. Furst, *Phys. Rev. E* **2009**, *79*, 050401; d) S. Noda, M. Yokoyama, M. Imada, A. Chuntinan, M. Mochizuki, *Science* **2001**, *293*, 1123; e) S. Bhaskar, J. Hitt, S. W. L. Chang, J. Lahann, *Angew. Chem.* **2009**, *121*, 4659; *Angew. Chem. Int. Ed.* **2009**, *48*, 4589; f) X. S. Wang, H. Guerin, H. Wang, Y. Wang, I. Manners, M. A. Winnik, *Science* **2007**, *317*, 644; g) J. F. Hulvat, S. I. Stupp, *Adv. Mater.* **2004**, *16*, 589; h) S. Bhaskar, K. M. Pollock, M. Yoshida, J. Lahann, *Small* **2010**, *6*, 404.

[4] a) A. van Blaaderen, *Science* **2003**, *301*, 470; b) V. N. Manoharan, M. T. Elseser, D. J. Pine, *Science* **2003**, *301*, 483; c) Q. Chen, S. C. Bae, S. Granick, *Nature* **2011**, *469*, 381.

[5] a) R. Costi, A. E. Saunders, U. Banin, *Angew. Chem.* **2010**, *122*, 4996; *Angew. Chem. Int. Ed.* **2010**, *49*, 4878; b) W. U. Huynh, J. J. Dittmer, A. P. Alivisatos, *Science* **2002**, *295*, 2425; c) Z. H. Nie, D. Fava, E. Kumacheva, S. Zou, G. C. Walker, M. Rubinstein, *Nat. Mater.* **2007**, *6*, 609.

[6] a) M. A. Horsch, Z. L. Zhang, S. C. Glotzer, *Phys. Rev. Lett.* **2005**, *95*, 056105; b) L. He, L. Zhang, Y. S. Ye, H. J. Liang, *J. Phys. Chem. B* **2010**, *114*, 7189.

[7] a) S. H. Park, J.-H. Lim, S. W. Chung, C. A. Mirkin, *Science* **2004**, *303*, 348; b) S. W. Kim, S. K. Kim, S. H. Park, *J. Am. Chem. Soc.* **2009**, *131*, 8380; c) S. R. Nicewarner-Pena, R. G. Freeman, B. D. Reiss, L. He, D. J. Pea, I. D. Walton, R. Cromer, C. D. Keating, M. J. Natan, *Science* **2001**, *294*, 137; d) M. Lahav, E. A. Weiss, Q. B. Xu, G. M. Whitesides, *Nano Lett.* **2006**, *6*, 2166; e) M. Lahav, T. Sehayek, A. Vaskevich, I. Rubinstein, *Angew. Chem.* **2003**, *115*, 5734; *Angew. Chem. Int. Ed.* **2003**, *42*, 5576; f) J. C. Love, A. R. Urbach, M. G. Prentiss, G. M. Whitesides, *J. Am. Chem. Soc.* **2003**, *125*, 12696.

[8] a) P. H. C. Camargo, Y. Xiong, L. Ji, M. J. Zuo, Y. Xia, *J. Am. Chem. Soc.* **2007**, *129*, 15452; b) Z. H. Lin, Y. W. Lin, K. H. Lee, G. T. Chang, *J. Mater. Chem.* **2008**, *18*, 2569.

[9] a) Y. Y. Wu, R. Fan, P. D. Yang, *Nano Lett.* **2002**, *2*, 83; b) M. S. Gudiksen, L. J. Lauhon, J. Wang, D. C. Smith, C. M. Lieber, *Nature* **2002**, *415*, 617.

[10] a) D. J. Milliron, S. M. Hughes, Y. Cui, L. Manna, J. B. Li, L. W. Wang, A. P. Alivisatos, *Nature* **2004**, *430*, 190; b) B. Koo, B. A. Korgel, *Nano Lett.* **2008**, *8*, 2490; c) L. F. Xi, C. Boothroyd, Y. M. Lam, *Chem. Mater.* **2009**, *21*, 1465.

[11] a) R. D. Robinson, B. Sadtler, D. O. Demchenko, C. K. Erdonmez, W. L. Wang, A. P. Alivisatos, *Science* **2007**, *317*, 355; b) D. Seo, C. Yoo, J. W. Jung, H. J. Song, *J. Am. Chem. Soc.* **2008**, *130*, 2940; c) J. B. Rivest, S. L. Swisher, L. K. Fong, H. M. Zheng, A. P. Alivisatos, *ACS Nano* **2011**, *5*, 3811.

[12] a) G. M. Whitesides, M. Boncheva, *Proc. Natl. Acad. Sci. USA* **2002**, *99*, 4769; b) N. Bowden, A. Terfort, J. Carbeck, G. M. Whitesides, *Science* **1997**, *276*, 233; c) G. M. Whitesides, J. P. Mathias, C. T. Seto, *Science* **1991**, *254*, 1312.

[13] a) Y. Lu, Y. Yin, Y. Xia, *Adv. Mater.* **2001**, *13*, 415; b) T. Ding, K. Song, K. Clays, C. H. Tung, *Adv. Mater.* **2009**, *21*, 1936; c) Z. X. Tang, R. W. Peng, D. Y. Fan, S. C. Wen, H. Zhang, L. J. Qian, *Opt. Express* **2005**, *13*, 9796.

[14] a) J. W. Ciszek, L. Huang, Y. Wang, C. A. Mirkin, *Small* **2008**, *4*, 206; b) J. W. Ciszek, L. Huang, S. Tsonchev, Y. H. Wang, K. R. Shull, M. A. Ratner, G. C. Schatz, C. A. Mirkin, *ACS Nano* **2010**, *4*, 259.

[15] a) J. H. Zhang, H. Y. Liu, Z. L. Wang, N. Y. Ming, *Chem. Eur. J.* **2008**, *14*, 4374; b) A. Kuijk, A. van Blaaderen, A. Imhof, *J. Am. Chem. Soc.* **2011**, *133*, 2346;c) J. He, M. J. Hourwitz, Y. J. Liu, M. T. Perez, Z. H. Nie, *Chem. Comm.* **2011**, *47*, 12450.

[16] Y. H. Wang, C. L. Zhang, C. Tang, J. Li, K. Shen, J. G. Liu, X. Z. Qu, J. L. Li, Q. Wang, Z. Z. Yang, *Macromolecules* **2011**, *44*, 3787.

[17] R. Y. Li, Y. Zhang, X. R. Zhou, X. L. Sun, *Chem. Phys. Lett.* **2008**, *458*, 138.
[18] a) A. G. Smallwood, P. S. Thomas, A. S. Ray, *Spectrochim. Acta Part A* **1997**, *53*, 2341; b) G. Orcel, L. L. Hench, I. Artaki, J. Jonas, T. W. Zerda, *J. Non-Cryst. Solids* **1988**, *105*, 223.
[19] J. H. Ryu, D. J. Hong, M. Lee, *Chem. Commun.* **2008**, 1043.
[20] a) D. E. Discher, A. Eisenberg, *Science* **2002**, *297*, 967; b) B. M. Discher, Y.-Y. Won, D. S. Ege, J. C.-M. Lee, F. S. Bates, D. E. Discher, D. A. Hammer, *Science* **1999**, *284*, 1143; c) D. J. Mitchell, B. W. Ninham, *J. Chem. Soc. Faraday Trans.* **1981**, *77*, 601; d) H. J. Kim, T. Kim, M. Lee, *Acc. Chem. Res.* **2011**, *44*, 72; e) M. Lee, B. K. Cho, K. J. Ihn, K. L. Lee, N. K. W. Oh, W. C. Zin, *J. Am. Chem. Soc.* **2001**, *123*, 4647; f) J. T. Chen, E. L. Thomas, C. K. Ober, G. P. Mao, *Science* **1996**, *273*, 343.
[21] a) C. R. Sides, C. R. Martin, *Mod. Aspects Electrochem.* **2007**, *40*, 75; b) K. T. Lee, J. Cho, *Nano Today* **2011**, *6*, 28.

